

RECENT HERA RESULTS ON PROTON STRUCTURE

AHARON LEVY

*Tel Aviv University, Tel Aviv, Israel
On behalf of the H1 and ZEUS collaborations*



The latest results of the two HERA collaborations, H1 and ZEUS, are presented. They include the most recent measurements of the longitudinal structure function F_L from both collaborations. Also presented are high Q^2 measurements from the ZEUS collaboration in the high Bjorken x region up to values of $x \cong 1$.

1 Introduction

HERA was a high-energy electron^e-proton collider, at a centre-of-mass (cms) energy of 320 GeV. It started operating in 1992 and was closed in 2007. Due to the accessible high values of virtuality, Q^2 , of the exchanged boson (see Fig. 1), reaching values up to about 40 000 GeV², it could 'look' into the proton with a resolution λ of about 10^{-3} fm.

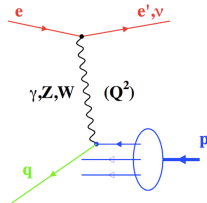


Figure 1 – Diagram describing ep collisions.

At HERA many experiments were performed by changing the virtuality of the exchanged photon from almost-real photons ($Q^2 \sim 0$), the photoproduction region, through the start of the deep inelastic scattering (DIS) region, $Q^2 \sim 4$ GeV² ($\lambda=0.1$ fm), to the very high- Q^2 region, $Q^2 \sim 40\,000$ GeV² ($\lambda = 10^{-3}$ fm), where electroweak physics could be studied.

In this talk, two of the most recent results concerning the proton structure will be presented. The first is a measurement^{1,2}, by both collaborations, of the longitudinal structure function, F_L . The second, carried out by the ZEUS collaboration³, is the high Q^2 measurements in the high Bjorken x region up to values of $x \cong 1$.

^aHere and in the following the term electron denotes generically both the electron and the positron.

2 Measuring the longitudinal structure function F_L

The F_L structure function was measured at HERA only during the last months of its running in 2007. Up to that time, measurements of the F_2 structure function were limited⁴ to low y , where y is the fraction of the lepton energy transferred to the proton in its rest frame. The coefficient in front of the F_L term is y^2 and thus its contribution to the cross section, compared to that of the F_2 structure function, is very small for low- y values.

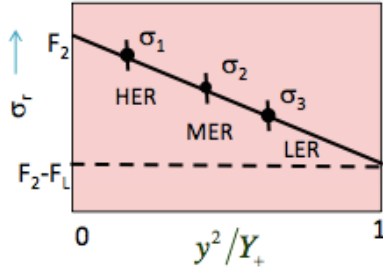


Figure 2 – A sketch of the linear dependence of σ_r on y^2/Y_+ . The intercept is F_2 and the slope gives F_L .

The reduced cross section, σ_r , can be expressed by two terms in the region where the Z exchange can be neglected, meaning Q^2 values far below the square of the Z mass,

$$\sigma_r = F_2(x, Q^2) - (y^2/Y_+)F_L(x, Q^2), \quad (1)$$

where $Y_+ = 1 + (1 - y)^2$. Measuring σ_r at different y but at the same x, Q^2 values gives a linear dependence of σ_r on y^2/Y_+ and therefore allows a simultaneous determination of the two structure functions F_2 and F_L . This is shown in Fig. 2. Since $y = Q^2/(xs)$, where s is the cms squared of the ep system, the way to vary y is to vary s . This has been done by changing the proton-beam energy to 460 and 575 GeV.

The determination of F_L needs the measurement of high- y events. The variable y is a function of the scattered electron kinematics,

$$y = 1 - \frac{E'}{E_e(1 - \cos \theta)}, \quad (2)$$

where E_e is the electron-beam energy, E' and θ are the energy and angle of the scattered electron, respectively. Thus high values of y means low E' of the scattered electron. Electron finders of both collaborations, prior to this measurement, were very well trained to identify scattered electrons with energies $E' > 10$ GeV. For lower energies, the efficiencies and purities of the finders deteriorate because of the photoproduction background. The ZEUS collaboration succeeded to improve their finder to allow to include in the F_L measurements events with $E' > 6$ GeV. The H1 collaboration, whose detector is better suited for this measurement could go down to $E' > 3$ GeV. Control plots showing a comparison between data and Monte Carlo for

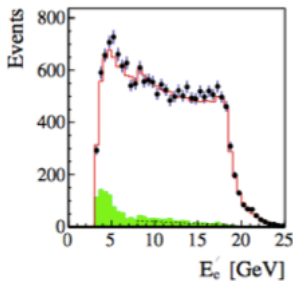


Figure 3 – Comparison of data and Monte Carlo for the scattered electron energy distribution at proton-beam energy of 460 GeV for the H1 collaboration. The shaded region is the photoproduction background.

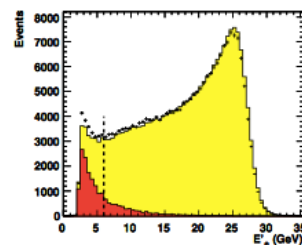


Figure 4 – Comparison of data and Monte Carlo for the scattered electron energy distribution at proton-beam energy of 460 GeV for the ZEUS collaboration. The dark-shaded region is the photoproduction background.

the E' variable for the low-energy run (proton beam of 460 GeV) are shown in Figs. 3 and 4.

The photoproduction background is shown in the dark-shaded region and is seen to increase sharply for low E' values.

Following the limitations on the energy of the scattered electron, the ZEUS collaboration measured F_L in the kinematic range $9 < Q^2 < 110 \text{ GeV}^2$ while the H1 collaboration covered the region $1.5 < Q^2 < 800 \text{ GeV}^2$. The results are shown in Fig. 5. The uncertainties of the ZEUS results are larger than those of H1. The ZEUS results, though consistently lower than those of H1, are consistent with them because of the correlated uncertainties. Taking into account the correlations between the ZEUS data points and neglecting the correlations between the H1 data points a χ^2 of 12.2 is obtained for 8 degrees of freedom. The predictions shown by the shaded area are in reasonable agreement with both data sets.

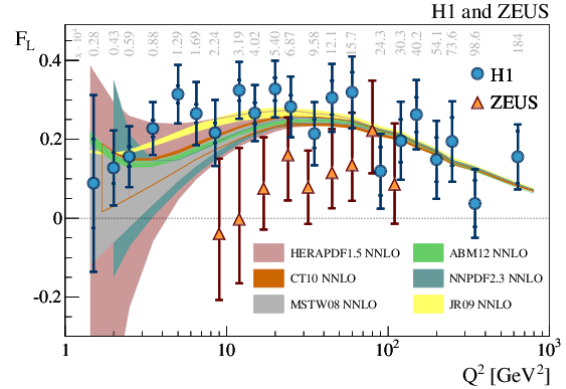


Figure 5 – F_L as a function of Q^2 as measured by the H1 and ZEUS collaborations. The shaded area are predictions based on different parameterisation, as indicated in the figure.

3 High x , extending to $x \cong 1$

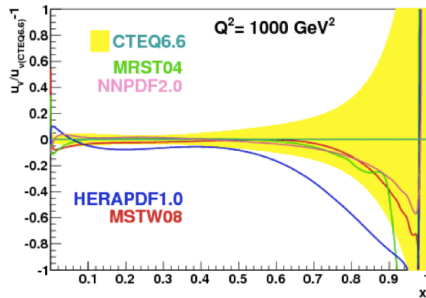


Figure 6 – Example of the sizable differences between some parameterisation description of the u valence quark, u_V .

The DIS cross sections have been measured by both collaborations with very high precision. These measurements were combined and produced text-book results with even higher precision⁵. Nevertheless, the highest x value for which measurements were done was 0.65. There are fixed-target experiments^{6,7,8} which measure higher values of x but in a low Q^2 region. In global perturbative quantum chromodynamic fits of parton distribution functions (PDFs), a parameterisation of the form $(1-x)^\beta$ is assumed in order to extend PDFs to $x = 1$. Although all fitters use the same parameterisation, sizeable differences are obtained in the high- x region⁹, as shown in Fig. 6.

The ZEUS collaboration showed in an earlier publication¹⁰ that the kinematics of HERA and the design of the detectors allow extension of the measurements of the neutral current (NC) cross sections up to $x = 1$. The results presented here are based on a much larger data sample and an improved analysis procedure.

A typical NC high- Q^2 and high- x event consists of the scattered electron and a high-energy collimated jet of particles in the direction of the struck quark. The electron and the jet are balanced in transverse momentum. The proton remnant mostly disappears down the beam pipe. The x and Q^2 of events, in which the jet is well contained in the detector, may be determined by various techniques. However, the maximum x value that can be reached is limited by the fact that at the low values of y typical of these events, the uncertainty on $x = Q^2/ys$ increases as $\Delta x \sim \Delta y/y^2$. An improved x reconstruction is achieved by observing that, in the limit of $x \rightarrow 1$, the energy of the struck quark represented by a collimated jet is $E_{\text{jet}} \cong xE_p$. The expression for x is

$$x = \frac{E_{\text{jet}}(1 + \cos \theta_{\text{jet}})}{2E_p \left(1 - \frac{E_{\text{jet}}(1 - \cos \theta_{\text{jet}})}{2E_e}\right)}, \quad (3)$$

where θ_{jet} is the scattering angle of the jet in the detector.

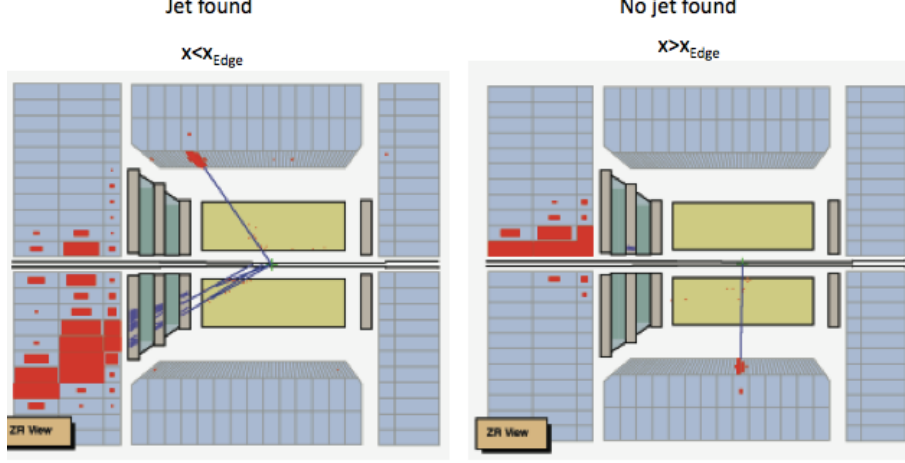


Figure 7 – Left-hand side: a one-jet event with a scattered electron in the BCAL and the jet fully contained in the FCAL. Also seen in FCAL are the proton remnant. Right-hand side: A zero-jet event where the scattered electron is in BCAL and the jet remains inside the beam pipe. The proton remnant and possibly some energy emerging from the jet in the beam pipe are seen in FCAL.

As x increases and the jet associated with the struck quark disappears down the beam-pipe (see Fig. 7), the ability to reconstruct x is limited by the energy loss. However, in these events, the cross section integrated from a certain limit in x , x_{edge} , up to $x = 1$ is extracted. The value of x_{edge} below which the jet is fully contained in the detector depends on Q^2 and the higher the Q^2 , the higher the value of x_{edge} .

The double-differential Born-level cross sections as a function of Q^2 and x have been measured in finer binning in x because of the large data samples in this analysis (53 099 for the e^-p and 37 361 for the e^+p sample). For the highest integrated x bin, the respective average cross sections, defined as

$$I(x) = \frac{1}{1 - x_{\text{edge}}} \int_{x_{\text{edge}}}^1 \frac{d^2\sigma(x, Q^2)}{dx dQ^2} dx, \quad (4)$$

have been obtained and plotted at $x = (x_{\text{edge}} + 1)/2$. The ratio of the measured cross sections to those expected from HERAPDF1.5¹¹ are shown in Figs. 8 and 9. Note that for bins where no events are observed, the limit is quoted at 68% probability, neglecting the systematic uncertainty. Also shown are the predictions from a number of other PDF sets (ABM11¹², CT10¹³, MSTW2008¹⁴, NNPDF2.3¹⁵), normalised to the predictions from HERAPDF1.5. Within the quoted uncertainties, the agreement between measurements and expectations is good.

4 Summary

Final measurements of the F_L structure functions are being published by HERA. The H1 collaboration covers a large kinematic range in Q^2 , $1.5 < Q^2 < 800 \text{ GeV}^2$. This is made possible by measuring scattered electrons down to 3 GeV due to good tracking and electromagnetic calorimetry in the rear direction. The results of the ZEUS collaboration in the Q^2 region covered by their measurements, $9 < Q^2 < 110 \text{ GeV}^2$, are in general lower than those of H1 but taking into account correlated uncertainties, are consistent with those of H1. Both results are consistent with expectations, though at low Q^2 there are large uncertainties in the theoretical predictions.

The ZEUS collaboration measured double-differential cross sections for $e^\pm p$ NC DIS events at $Q^2 > 725 \text{ GeV}^2$ up to $x \cong 1$. Fine binning in x and extension of kinematic coverage up to $x \cong 1$ make the data important input to fits constraining the PDFs in the valence-quark domain.

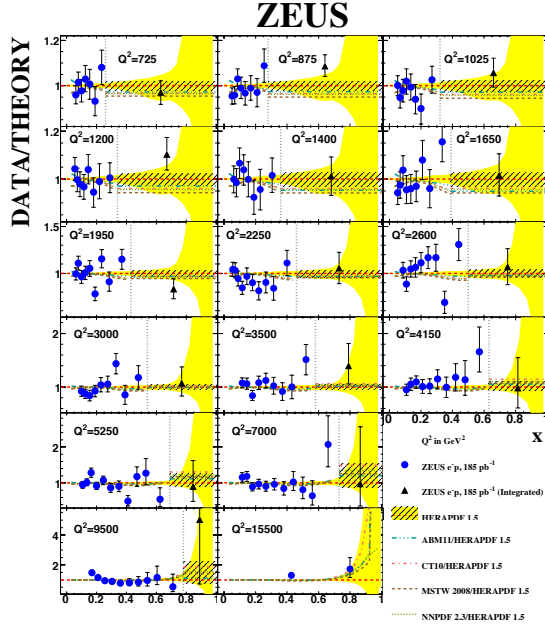


Figure 8 – Ratio of the double-differential cross section for NC e^-p scattering and of the double-differential cross section integrated over x to the Standard Model expectation evaluated using the HERAPDF1.5 PDFs as a function of x at different Q^2 values as described in the legend. For HERAPDF1.5, the uncertainty is given as a band. The expectation for the integrated bin is also shown as a hatched box. The error bars show the statistical and systematic uncertainties added in quadrature. The expectations of other commonly used PDF sets normalised to HERAPDF1.5 PDFs are also shown, as listed in the legend. Note that the scale on the y axis changes with Q^2 .

Acknowledgments

This activity was partially supported by the Israel Science Foundation.

References

1. H1 Collaboration, V. Andreev et al., Eur. Phys. J. **C 74** (2014) 2814.
2. ZEUS Collaboration, H. Abramowicz et al., DESY-14-053.
3. ZEUS Collaboration, H. Abramowicz et al., Phys. Rev. **D 89** (2014) 072007.
4. See e.g. H. Abramowicz and A. Caldwell, Rev. Mod. Phys. **71** (1999) 1275.
5. H1 and ZEUS Collaborations, F.D. Aaron et al., JHEP **1001** (2010) 109.
6. BCDMS Collaboration, A.C. Benvenuti et al., Phys. Lett. **B 223** (1989) 485.
7. L.W. Whitlow et al., Phys. Lett. **B 282** (1992) 475.
8. S.P. Malace et al., Phys. Rev. **C 80** (2009) 035207.
9. A. Caldwell for the ZEUS Collaboration, *Measurement of positron-proton neutral current cross sections at high Bjorken- x with the ZEUS detector at HERA*, presented at the EPS2013, Stockholm, July 2013.
10. ZEUS Coll., S. Chekanov et al., Eur. Phys. J. **C 49** (2007) 523.
11. V. Radescu, *Combination of QCD Analysis of the HERA Inclusive Cross Sections*, arXiv: 1308.0374 [hep-ex] (2013).
12. S. Alekhin, J. Blümlein and S.O. Moch, PoS **LL2012** (2012) 016.

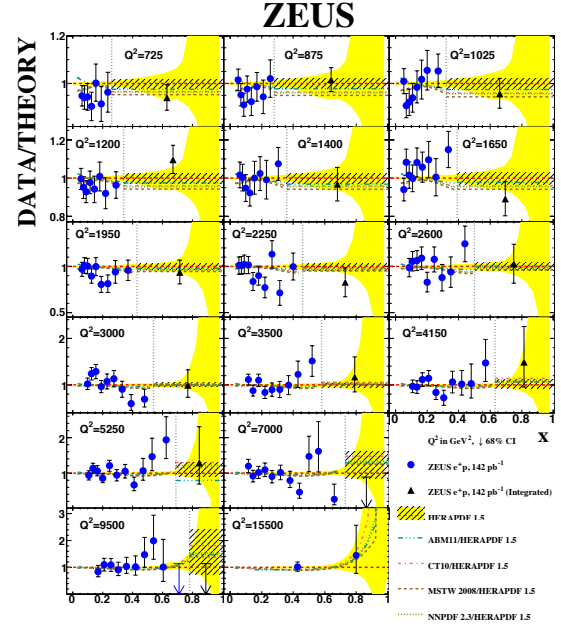


Figure 9 – Ratio of the double-differential cross section for NC e^+p scattering and of the double-differential cross section integrated over x to the Standard Model expectation evaluated using the HERAPDF1.5 PDFs as a function of x at different Q^2 values as described in the legend. For HERAPDF1.5, the uncertainty is given as a band. The expectation for the integrated bin is also shown as a hatched box. The error bars show the statistical and systematic uncertainties added in quadrature. The expectations of other commonly used PDF sets normalised to HERAPDF1.5 PDFs are also shown, as listed in the legend. Note that the scale on the y axis changes with Q^2 .

13. M. Guzzi et al., *CT10 parton distributions and other developments in the global QCD analysis*, SMU-HEP-10-11 (2011), arXiv: 1101.0561 [hep-ph] (2011).
14. A.D. Martin et al., Eur. Phys. J. **C 63** (2009) 189.
15. R. Ball et al., JHEP **1304** (2013) 125.